The surfaces of Ti and Nano-Ti were observed using a scanning electron microscope (SEM: JSM-6380LA, JEOL Ltd., Tokyo, Japan) and an atomic force microscope (AFM: VN-8000, Keyence Co., Osaka, Japan). Scanning area of AFM observation was 2.5 μm x 2.5 μm. With the AFM observation, the surface characteristics such as pitch, ridge width, depth, and surface roughness were also determined using an analytical software equipped in the AFM. Three specimens (n=3) were prepared for each group, and measurement was performed at five different points in each specimen.

2.3 Isolation and cultivation of human synovium-derived mesenchymal stem cells

Human synovial membranes were obtained aseptically from the knee joints of patients during knee surgery on an agreement of tissue harvest. The method for the isolation and cultivation of human synovium-derived mesenchymal stem cells are described elsewhere.[15-17] Briefly, the synovial membrane specimens were rinsed with a phosphate buffered saline (PBS(-)) solution, minced meticulously, and digested with 0.1% type IV collagenase (Sigma-Aldrich Co., St. Louis, MO, USA) for 1.5 h at 37°C. After neutralization of the collagenase with growth medium containing high-glucose Dulbecco's modified Eagle's medium (Gibco BRL, Life Technologies Inc., Rockville, MD, USA) supplemented with 10% fetal bovine serum (FBS; Nichirei Biosciences Inc., Tokyo, Japan) and antibiotic (100 U/mL penicillin and 100 μg/mL streptomycin, Gibco BRL, Life Technologies Inc.), the cells were collected by centrifugation, washed with a PBS(-) solution, resuspended in growth medium, and plated in the tissue culture treated polystyrene dishes. The cells were cultured in the growth medium at 37°C in a humidified atmosphere of 5% CO_2. The medium was replaced once per week. After 14 d of primary cultivation, when the cells reached 80-100% confluence, they were washed twice with a PBS(-) solution, harvested by treatment with a trypsin-EDTA solution

(0.25% trypsin and 1 mM EDTA: Gibco BRL, Life Technologies Inc.), and replated at 1/5 dilutions for the first subculture. Cell passages were continued in the same manner with 1/5 dilutions when cultures reached near 100% confluence. The procedure of tissue harvest and subsequent cell culture were approved by the institutional review boards of Osaka University Medical School and Kogakuin University. Moreover, all procedures of this study followed the Declaration of Helsinki Principles.

Each titanium specimen was sterilized by autoclaving with reverse osmosis water and then placed on non-treated 12-well polystyrene dishes (22.1 mmφ). Then, the cells at 4-time passage were seeded on each specimen at a density of 3.0×10^3 cells/cm^2 and cultured for 1 h, 6 h, and 24 h.

2.4 Cellular attachment assays

For fluorescence microscopic observation, actin filaments, vinculin, and nuclei were stained. The cells were fixed with 4% paraformaldehyde solution. Nonspecific binding of the antibody was blocked by a blocking solution containing 5% goat serum in PBS(-) solution supplemented with 0.5% Tween20. The cells were reacted with monoclonal anti-vinculin (mouse IgG1 isotype) (Sigma-Aldrich Co.). Then, they were labeled with Alexa Fluor® 488-conjugated goat anti-mouse isotype-specific antibodies (Life Technologies Co., Carlsbad, CA, USA) and 0.7% rhodamine/phalloidin (Cytoskeleton Inc., Denver, CO, USA). Finally, nuclei were stained with 0.5% Hoechst33342 (Dojindo Laboratories Inc., Kumamoto, Japan). They were then observed using a fluorescence microscope (IX-7, Olympus Co., Tokyo, Japan).

For scanning electron microscopic (SEM) observation, the primary fixation of the cells on each specimen was performed by Karnovsky's fixative.[18] The secondary fixation was

performed using a 1% osmium tetraoxide solution. They were then gradually dehydrated in 50, 70, 80, 90, 95, and 100% ethanol, in increasing order, and dried in the CO_2 critical point drier. The cells on the specimens were then observed using a SEM (JSM-6380LA, JEOL Ltd.). The morphological parameters of the cells such as adhesion area, aspect ratio, and orientation angle were determined with ImageJ software (version 1.46, National Institutes of Health (NIH)). The outline of a cell in the SEM image was drawn and then the area of contoured part was calculated as cellular adhesion area. For the quantitative determinations of the aspect ratio and the orientation angle of the cell, the elliptical approximation of each cell was initially carried out on the SEM images.[19] The aspect ratio was calculated by dividing the elliptical long axis by its short axis. The orientation angle of the long axis of the cell with respect to the direction of the groove on Nano-Ti was calculated. The orientation angle on Ti was defined as the angle between the long axis of a cell and an arbitrary line. Ten cells on each specimen were analyzed to obtain average values for the adhesion area and aspect ratio. Fifty cells on each specimen were analyzed for the orientation angle.

2.5 Statistical analysis

All data were presented as mean ± standard deviation and were analyzed using the Student's two-tailed *t*-test with a significance level set at $P < 0.05$.

3. Results

3.1 Surface observation and characterization

Results of scanning electron microscopic observation are shown in Fig.1 while results of atomic force microscopic observation are shown in Fig.2. Region of interest for observation was randomly selected for each specimen. The surface geometry due to polish treatments with SiC papers was observed on Ti. On the other hand, the nano-sized periodic structure was observed on Nano-Ti surface. The orientation of the incident beam polarization was indicated in Fig.1d. The nano-periodic structure on the Nano-Ti exhibited 501 ± 100 nm of pitch, 99 ± 31 nm of depth, and 292 ± 50 nm of ridge. The parameters of surface roughness determined with AFM image data; the values of R_a, R_q, R_z, and R_v, were summarized in Table I. The roughness parameters of Nano-Ti were approximately 2-3 times higher than those of Ti.

3.2 Cell attachment, extension, and anisotropy

Results of fluorescence microscopic observation of cells cultured on Ti and Nano-Ti were shown in Figs.3, 4, and 5, respectively. Actin filament: a protein of cytoskeleton, vinculin: a membrane-cytoskeletal protein connecting integrin to actin cytoskeleton in focal adhesion plaques[20,21], and nucleus were indicated in a and e, b and f, and c and g, respectively. Composite images of actin filament, vinculin, and nucleus are shown in d and h. Note that the upper column (a, b, c, d) indicate cells on Ti while the lower column (e, f, g, h) indicate cells on Nano-Ti. The micrographs of cells cultured for 1 h and 6 h indicated that actin filaments and vinculin were more spread on Nano-Ti as compared with on Ti. It is, therefore, suggested that the cells on Nano-Ti exhibited more broad adhesion area than those on Ti at 1 h and 6 h of culture time (Figs.3 and 4). On the other hand, no significant differences in terms of the cell attachment and extension were observed at 24 h of culture time (Fig.5).

Scanning electron microscopic observation of cells cultured on Ti and Nano-Ti for 1 h, 6 h,

and 24 h were shown in Figs.6 and 7. The low magnification images showed that a cell cultured for 1 h on Nano-Ti was already extended (Fig.6d), though a cell shape on Ti was still spherical (Fig.6a). Moreover, the extension of a cell cultured for 6 h on Nano-Ti was greater than that on Ti (Figs.6b and 6e). In contrast, no significant difference in cell extension was observed between Ti and Nano-Ti at 24 h of culture time (Figs.6c and 6f). The high magnification images (Fig.7) showed that the fillopodia and lamellipodia of a cell had already extended on Nano-Ti at 1 h, though those on Ti had not been observed yet. Moreover, fillopodia and lamellipodia of the cell on Nano-Ti were extended more actively than those on Ti at 6 h. However, the fillopodia and lamellipodia of the cell on Ti were extended more actively than those on Nano-Ti at 24 h. Note that the fillopodia and lamellipodia of the cells on Nano-Ti were extended along the direction of grooves at 6 h and 24 h.

The adhesion areas of cells cultured for 1 h, 6 h, and 24 h are shown in Fig.8. The adhesion areas of cells cultured on Nano-Ti were significantly larger than those on Ti at 1 h and 6 h. However, no significant difference was observed in the areas of cells between Ti and Nano-Ti groups at 24 h. The aspect ratios of cells cultured for 1 h, 6 h, and 24 h are shown in Fig.9. The aspect ratio of cells on Nano-Ti was significantly higher than that on Ti at 6 h, though there were no significant difference in the aspect ratio between Ti and Nano-Ti groups at 1 h and 24 h. The orientation angles of cells cultured for 24 h are shown in Fig.10. Seventy eight percent of cells were distributed between −30° and 30°, and moreover, fifty percent of cells were distributed between −10° and 10° in Nano-Ti group. On the other hand, the orientation angles of cells were inconsistent in Ti group.

4. Discussion

Laser beam irradiation to a metallic substrate at an intensity around ablation threshold forms

nanoscopic levels of a periodic structure which is shaped like a grating. It has been reported that the threshold for forming a nano-periodic structure is approximately 0.1-1.0 J/cm^2.[22] In this study, a nano-periodic structure could not be patterned stably when the laser with the intensity of 0 mW was irradiated to a substrate at the focal point, because the laser intensity was fluctuated about 20 mW even if it was set at 0 mW. The diameter of condensing point is 15 μm when the laser was focused to the focal point. Therefore, the fluence of laser beam is 11.3 J/cm^2 when the laser intensity was 20 mW. This value of fluence was too strong to form a nano-periodic structure. Therefore, the laser was defocused for 7 mm from the focal point and the laser intensity was set at 700 mW. As a result, a nano-periodic structure was patterned stably. The fluence of laser beam became 0.203 J/cm^2 since the diameter of condensing point changes to 700 μm by defocusing. This value is in the range of threshold which allows to form a nano-periodic structure. In addition, the fluctuation of laser intensity at 700 mW with defocusing was smaller than those at 0 mW with focusing. Therefore, these laser irradiation conditions were suitable to pattern a nano-periodic structure stably on a titanium surface.

The formed pitch (501 ± 100 nm) was smaller than the wavelength of 780 nm of the nano-periodic structure. This result agreed well with a previous finding: the pitch (700 nm) was smaller than the wavelength (1,030 nm) in a femtosecond laser processing on titanium.[13] Similar tendency has been obtained on other substrates such as a copper, silicon wafer, and single crystals of MgF_2, BaF_2 and CaF_2.[14,22-24] However, the detailed mechanism of the tendency of laser processing has not been clarified. The surface roughness may be a factor which affects the processed pitches. In addition, the surface of pure titanium is stabilized by forming a thin oxide film of approximately 2-5 nm in thickness consisting of TiO_2, TiO, and Ti_2O_3.[25,26] The thin oxide film may affect the process of the nano-periodic structure. Further analyses and consideration as regard with factors affecting laser processing are

required.

In both the fluorescence microscopic and scanning electron microscopic observations (Figs.3, 4, 5, 6, and 7), the cells cultured on Nano-Ti extended over broader area than those on Ti at 1 h. The tendency similar to the cells cultured for 1 h was obtained in the cells cultured for 6 h. On the other hand, no significant difference was observed in terms of cell extension between the Ti and Nano-Ti groups at 24 h. The cells exhibited spherical shape at first, and then, they extended gradually after contacting on a material surface, and finally, they became spindle-shape. In general, cell adhesion and extension are completed sufficiently within 24 h, as shown in Fig.8. Although the cells were round-shape in both the Ti and Nano-Ti groups at 1 h of culture, they gradually became spindle-shape in the Nano-Ti group while they remained unchanged in the Ti group at 6 h of culture. Finally, the cells became spindle-shape in both the groups at 24 h of culture as shown in Fig.9. Therefore, it was indicated that Nano-Ti promoted the process of cell adhesion and extension. When the cells attach to and extend on the substrate, they spread their fillopodia and lamellipodia.[27] The extension occurred earlier around 1 h, continued around 6 h, and almost completed by 24 h in the Nano-Ti group as found in Fig.8. However, the extension occurred around 6 h, and still continued at 24 h in the Ti group. These results also suggest that Nano-Ti promoted the process of cell extension.

Fig.10 showed that the approximately 80% of cells on Nano-Ti were distributed within ± 30° with respect to the direction of nano-patterned grooves. Moreover, fillopodia and lamellipodia of cells on Nano-Ti spread along grooves. These results clearly indicated that Nano-Ti promoted the process of cell orientation. Results of the AFM observation and analysis indicated that the pitch, ridge width, and depth of Nano-Ti were 501 ± 100 nm, 292 ± 50 nm, and 99 ± 31 nm, respectively. It has been reported that the fibroblast alignment was promoted on groove ridge width larger than 100 nm.[28] In addition, it has been reported that

mesenchymal stem cells could recognize the grooves that were deeper than 90 nm.[29] Nano-Ti surface processed in this study fulfills all of these parameters. Therefore, Nano-Ti patterned in this study was suitable for cell adhesion, extension, and orientation.

5. Conclusions

In the present study, morphological observations were performed on human synovium-derived mesenchymal stem cells cultured on a nano-periodic patterned titanium structure processed using a femtosecond laser system. Results reveal that the patterned structure promotes the adhesive and anisotropic properties of the cells. It is suggested that the femtosecond laser processing technique is useful for the development and modification of cell-based biomaterials.

Acknowledgements

The present study was financially supported in part by the MEXT-Supported Program for the Strategic Research Foundation at Private Universities, 2008-2012 (BERC, Kogakuin University).

References

1) J. Y. Martin, Z. Schwartz, T. W. Hummert, D. M. Schraub, J. Simpson, J. Lankford Jr, D. D. Dean, D. L. Cochran, and B. D. Boyan: J. Biomed. Mater. Res. **29** (1995) 389.

2) K. Kieswetter, Z. Schwartz, T. W. Hummert, D. L. Cochran, J. Simpson, D. D. Dean, and B. D. Boyan: J. Biomed. Mater. Res. **32** (1996) 55.

3) B. D. Boyan, R. Batzer, K. Kieswetter, Y. Liu, D. L. Cochran, S. Szmuckler-Moncler, D. D. Dean, and Z. Schwartz: J. Biomed. Mater. Res. **39** (1998) 77.

4) L. Zhang, V. M. Menendez-Flores, N. Murakami, and T. Ohno: Appl. Surf. Sci. **258** (2012) 5803.

5) S. Ban, Y. Iwaya, H. Kono, and H. Sato: Dent. Mater. **22** (2006) 1115.

6) H. Asoh, K. Uchibori, and S. Ono: Semicond. Sci. Tech. **26** (2011) 102001.

7) H. Asoh, F. Arai, and S. Ono: Electrochim. Acta **54** (2009) 5142.

8) D. Z. Xie, B. K. A. Ngoi, Y. Q. Fu, A. S. Ong, and B. H. Lim: Appl. Serf. Sci. **225** (2004) 54.

9) S. Rennon, L. Bach, H. König, J. P. Reithmaier, A. Forchel, J. L. Gentner, and L. Goldstein: Microelectron. Eng. **57-58** (2001) 891.

10) A. I. Teixeira, G. A. Abrams, P. J. Bertices, C. J. Murphy, and P. F. Nealey: J. Cell Sci. **116** (2003) 1881.

11) Y. B. Xiao, E. H. Kim, S. M. Kong, J. H. Park, B. C. Min, and C. W. Chung: Vacuum **85** (2010) 434.

12) K-H. Leitz, B. Redlingshöfer, Y. Reg, A. Otto, and M. Schmidt: Phys. Procedia **12** (2011) 230.

13) V. Oliveira, S. Ausset, and R. Vilar: Appl. Surf. Sci **255** (2009) 7556.

14) J. Reif, O. Varlamova, and F. Costache: J. Appl. Phys. **92** (2008) 1019.

15) W. Ando, K. Tateishi, D. A. Hart, D. Katakai, Y. Tanaka, K. Nakata, J. Hashimoto, H. Fujie, K. Shino, H. Yoshikawa, and N. Nakamura: Biomaterials **28** (2007) 5462.

16) W. Ando, K. Tateishi, D. Katakai, D. A. Hart, C. Higuchi, K. Nakata, J. Hashimoto, H. Fujie, K. Shino, H. Yoshikawa, and N. Nakamura: Tissue Eng. Part A **14** (2008) 2014.

17) K. Shimomura, W. Ando, K. Tateishi, R. Nansai, H. Fujie, D. A. Hart, H. Kohda, K. Kita, T. Kanamoto, T. Mae, K. Nakata, K. Shino, H. Yoshikawa, N. Nakamura: Biomaterials **31** (2010) 8004.

18) M. J. Karnovsky: J. Cell Biol. **27** (1965) 137A.

19) S. Fujita, M. Ohshima, and H. Iwata: J. R. Soc. Interface **6** (2009) S269.

20) D. R. Critchley: Biochem. Soc. Trans. **32** (2004) 831.

21) V. E. Koteliansky, E. P. Ogryzko, N. I. Zhidkova, P. A. Weller, D. R. Critchley, K. Vancompernolle, J. Vandekerckhove, P. Strasser, M. Way, M. Gimona, and J. V. Small: Biochem. Eur. J. Biochem. **204** (1992) 767.

22) S. Sakabe, M. Hashida, S. Tokita, S. Namba, and K. Okamuro: Phys. Rev. B **79** (2009) 033409.

23) F. Costache, M. Henyk, J. Reif: Appl. Surf. Sci. **208-209** (2003) 486-491.

24) D. V. Tran, H. Y. Zheng, Y. C. Lam, V. M. Murukeshan, J. C. Chai, and D. E. Hardt: Opt. Lasers Eng. **43** (2005) 977.

25) K. Oya, Y. Tanaka, Y. Moriyama, Y. Yoshioka, T. Kimura, Y. Tsutsumi, H. Doi, N. Nomura, K. Noda, A. Kishida, and T. Hanawa: J. Biomed Mater. Res. A **94** (2010) 611.

26) Y. Tsutsumi, D. Nishimura, H. Doi, N. Nomura, and T. Hanawa: Mater. Sci. Eng. C **29** (2009) 1702.

27) B. Alberts, A. Johnson, J. Lewis, M. Raff, K. Roberts, and P. Walter: *Mol. Biol. Cell* (Garland Science, Abingdon, UK, 2008) 5th ed., p.996, 1006, 1037, 1040, and 1041.

28) W. A. Loesberg, J. te Riet, F. C. M. J. M. van Delft, P. Schon, C. G. Figdor, S. Speller, J.

J. W. A. van Loon, X. F. Walboomers, and J. A. Jansen: Biomaterials **28** (2007) 3944.

29) S. Fujita, D. Ono, M. Ohshima, H. Iwata: Biomaterials **29** (2008) 4494.

Figure Captions

Figure 1 SEM images of Ti (a, c) and Nano-Ti (b, d). Low magnification images (a, b) with scale bars of 10 μm, and high magnification images (c, d) with scale bars of 1 μm. The arrow in the image (d) indicates the orientation of the incident beam polarization.

Figure 2 AFM images of Ti (a) and Nano-Ti (b) with scanning area of 2.5 μm x 2.5 μm.

Figure 3 (Color) Fluorescence micrographs of cells cultured on Ti (a-d) and Nano-Ti (e-h) for 1 h. Actin filaments (a, e), vinculin (b, f), nuclei (c, g), and merged images (d, h) are shown with scale bars of 50 μm.

Figure 4 (Color) Fluorescence micrographs of cells cultured on Ti (a-d) and Nano-Ti (e-h) for 6 h. Actin filaments (a, e), vinculin (b, f), nuclei (c, g), and merged images (d, h) are shown with scale bars of 50 μm.

Figure 5 (Color) Fluorescence micrographs of cells cultured on Ti (a-d) and Nano-Ti (e-h) for 24 h. Actin filaments (a, e), vinculin (b, f), nuclei (c, g), and merged images (d, h) are shown with scale bars of 50 μm.

Figure 6 Low magnification SEM images of cells cultured on Ti (a, b, c) and Nano-Ti (d, e, f) for 1 h (a, d), 6 h (b, e), and 24 h (c, f) with scale bars of 5 μm (a, b, d, e) and 10 μm (c, f).

Figure 7 High magnification SEM images of cells cultured on Ti (a, b, c) and Nano-Ti (d, e, f) for 1 h (a, d), 6 h (b, e), and 24 h (c, f) with scale bars of 1 μm.

Figure 8　Cell adhesion areas on Ti and Nano-Ti cultured for 1 h, 6 h, and 24 h. Averaged data from 10 samples (n=10) are shown with standard deviation, with statistically significant differences set at 0.05.

Figure 9　Aspect ratios of adhered cells on Ti and Nano-Ti cultured for 1 h, 6 h, and 24 h. Averaged data from 10 samples (n=10) are shown with standard deviation, with statistically significant differences set at 0.05. The dotted line is just "1" indicating a shape of true circle.

Figure 10　Distribution of cells in the range of each orientation angle cultured for 24 h on Ti (a) and Nano-Ti (b) with sample number of 50 (n=50).

Table I Roughness parameters on Ti and Nano-Ti.

	Ra (nm)	Rq (nm)	Rz (nm)	Rv (nm)
Ti	20 ± 7	54 ± 21	155 ± 64	100 ± 48
Nano-Ti	57 ± 18	190 ± 54	390 ± 72	201 ± 34

The data are mean ± SD; n=3. Five points per specimen were measured.

Figure1

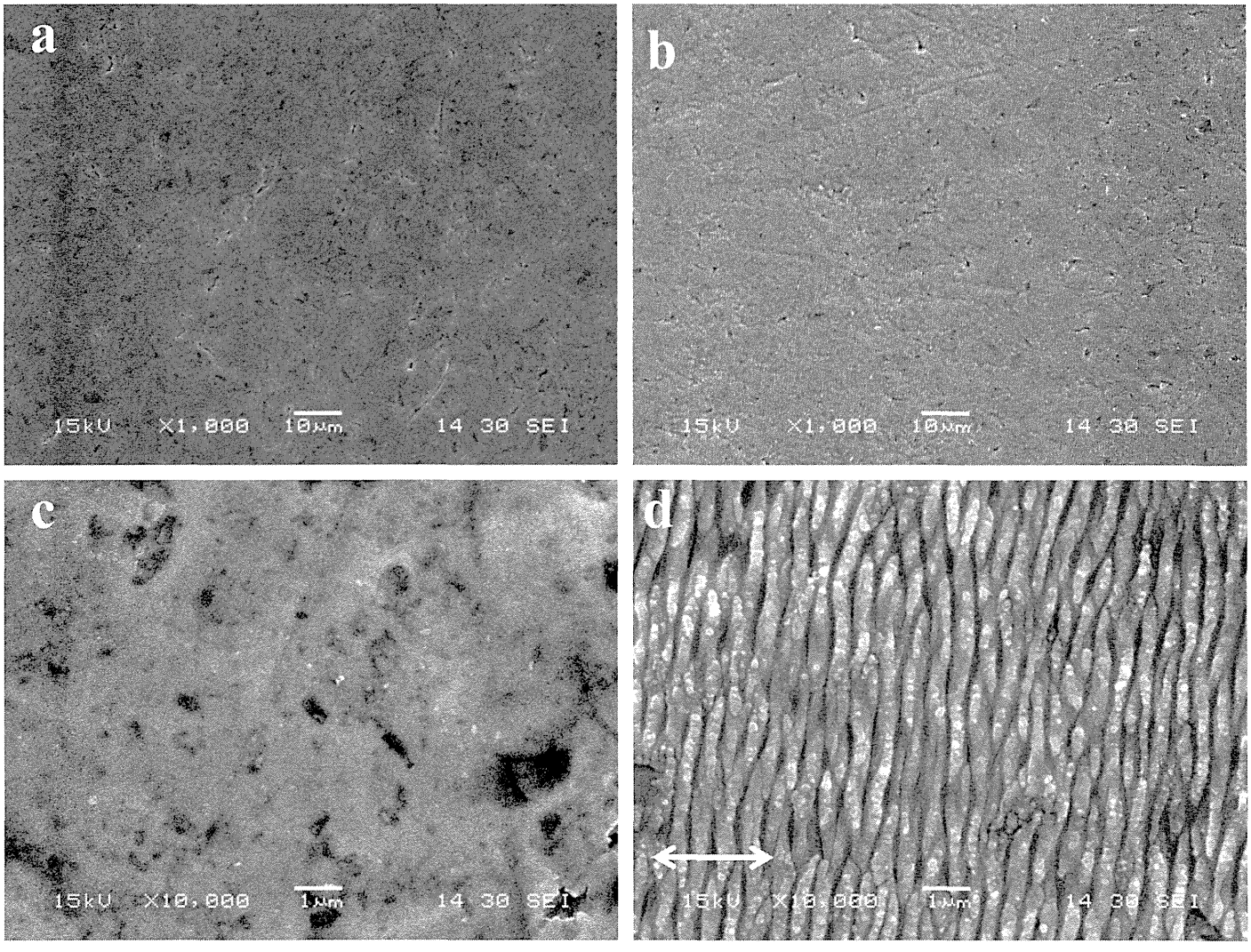
a
15kV X1,000 10μm 14 30 SEI
b
15kV X1,000 10μm 14 30 SEI
c
15kV X10,000 1μm 14 30 SEI
d
15kV X10,000 1μm 14 30 SEI

Figure2

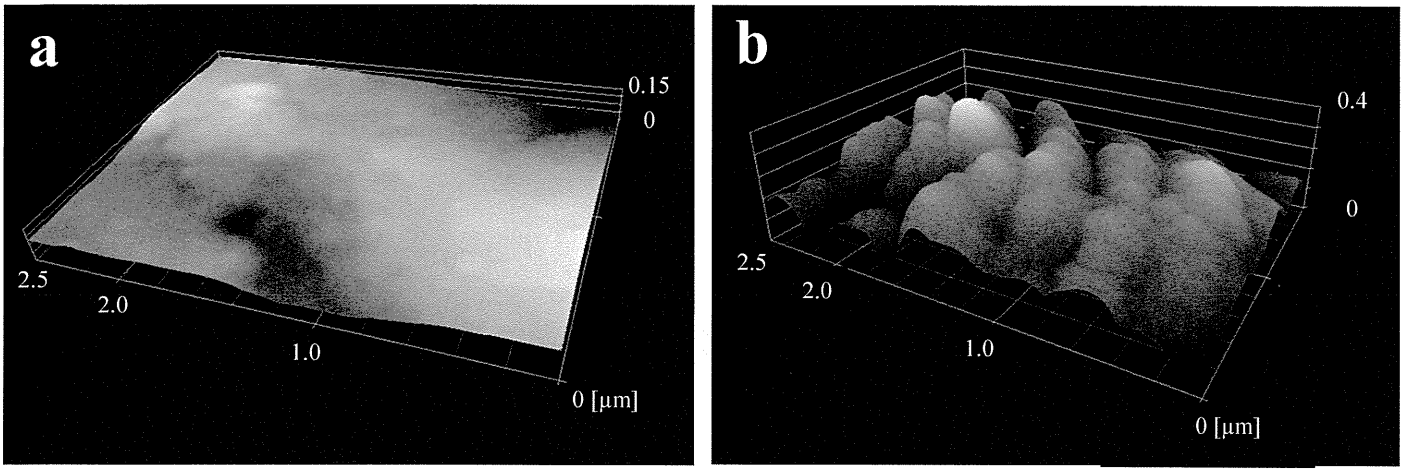

Figure3

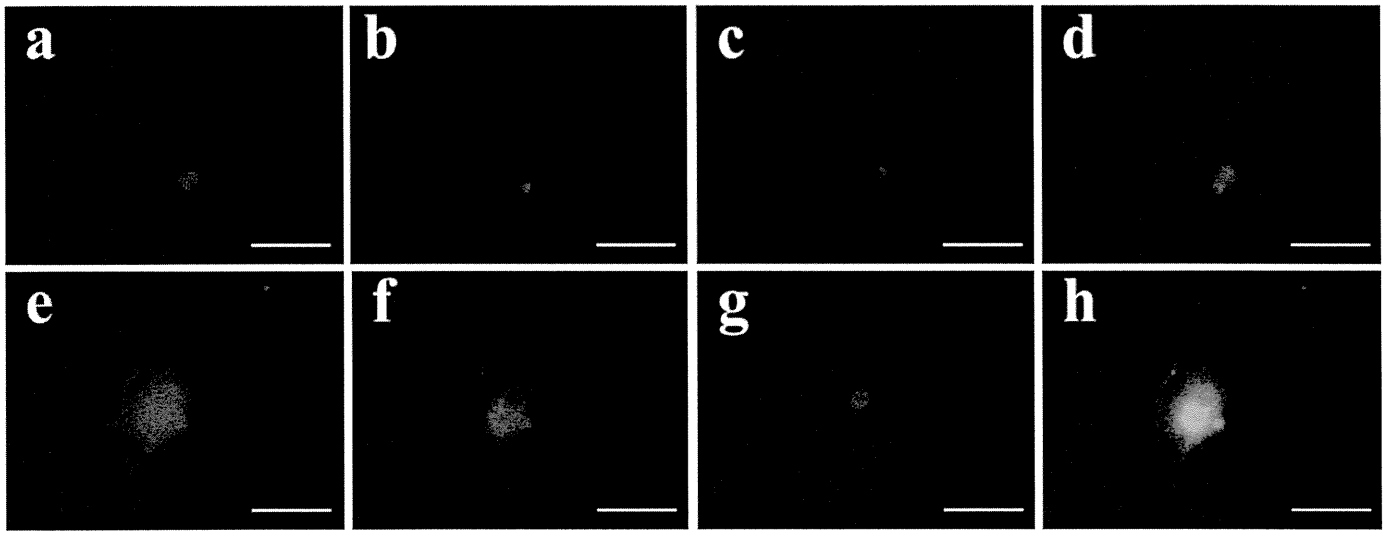

カラー印刷希望

Figure4

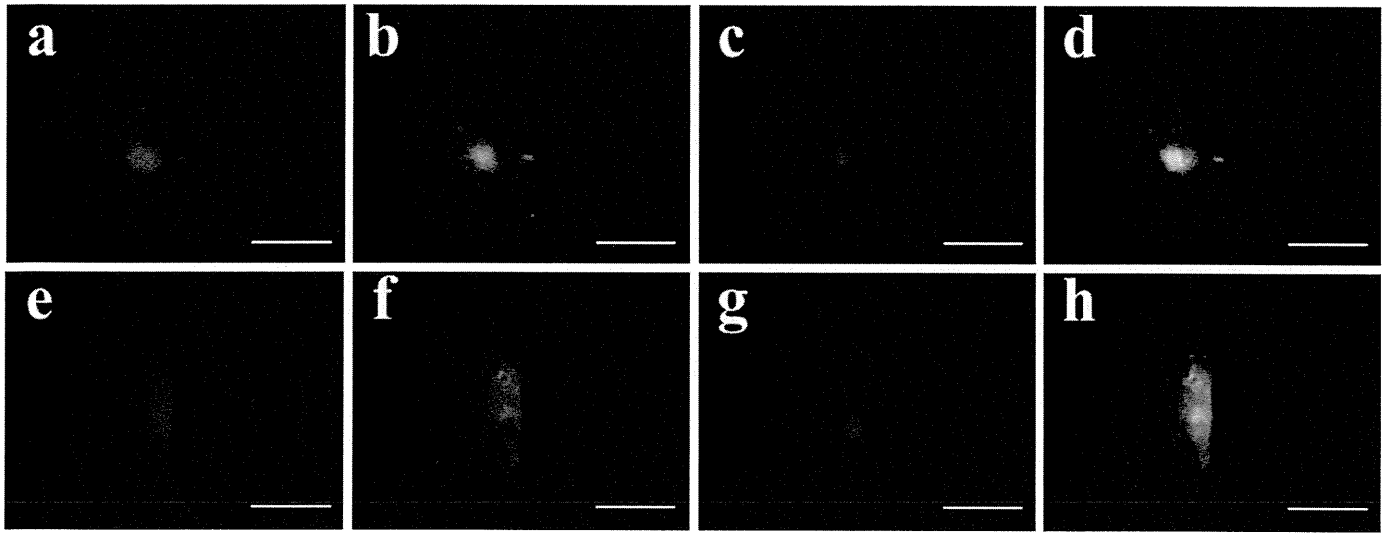

カラー印刷希望

Figure5

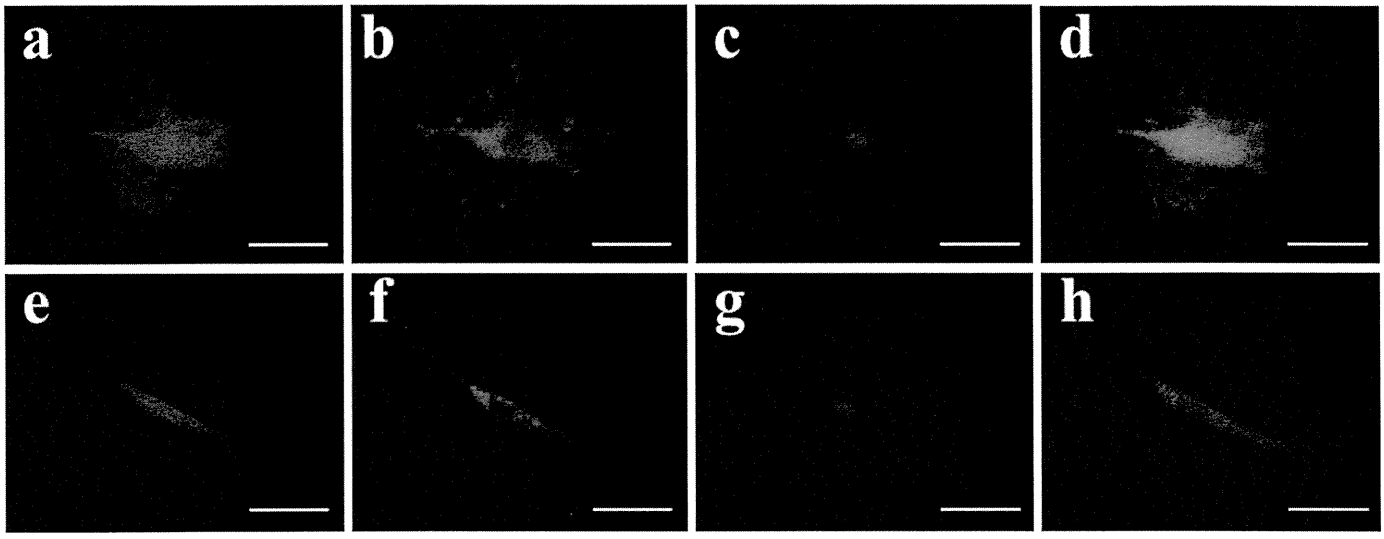

カラー印刷希望

Figure6

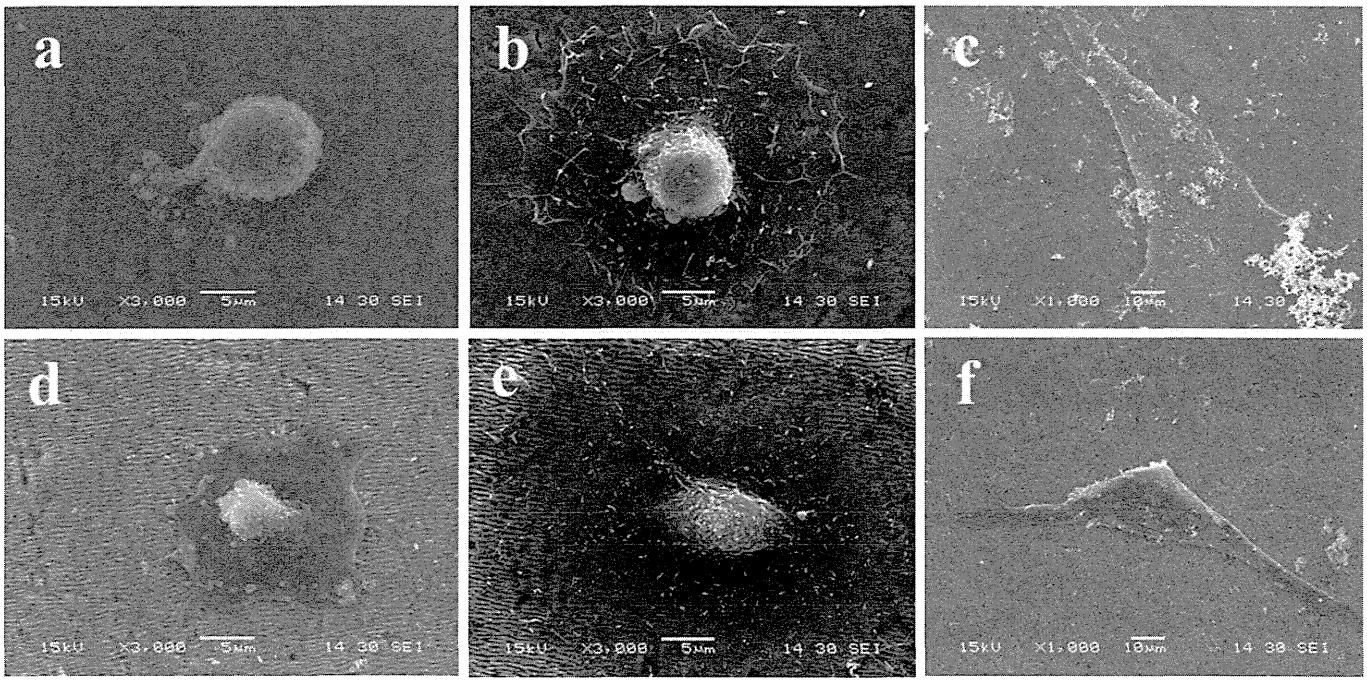
a
15kV X3,000 5μm 14 30 SEI
b
15kV X3,000 5μm 14 30 SEI
c
15kV X1,000 10μm 14 30 SEI
d
15kV X3,000 5μm 14 30 SEI
e
15kV X3,000 5μm 14 30 SEI
f
15kV X1,000 10μm 14 30 SEI